

PERIODIC MIXED CONVECTION FLOW ALONG THE SURFACE OF A THERMALLY AND ELECTRICALLY CONDUCTING CONE

by

Asifa ILYAS* and Muhammad ASHRAF

Department of Mathematics, Faculty of Science, University of Sargodha, Sargodha, Pakistan

Original scientific paper
<https://doi.org/10.2298/TSCI20S1225I>

The main aim of the present work is to highlight the significances of periodic mixed convection flow and heat transfer characteristics along the surface of magnetized cone by exerting magnetic field exact at the surface of the cone. The numerical simulations of coupled non-dimensional equations are computed in terms of velocity field, temperature and magnetic field concentration and then used to examine the periodic components of skin friction, τ_w , heat transfer, q_w , and current density, j_w , for various governing parameters. A nice periodic behavior of heat transfer q_w is concluded for each value of mixed convection parameter, λ , but maximum periodicity is sketched at $\lambda = 50$. It is also computed that the lower value of magnetic Prandtl number $\gamma = 0.1$ gets poor amplitude in current density but highest amplitude is sketched for higher $\gamma = 0.5$. The behavior of heat and fluid-flow in the presence of aligned magnetic field is associated with the phase angle and amplitude of oscillation. It is also noted that due to the increase in magnetic force parameter, ξ , there are wave like disturbances generate within the fluid layers. These disturbances are basically hydromagnetic waves which becomes more prominent as the strength of magnetic force parameter is increased.

Key words: *thermally and electrically conducting cone, periodic, current density, mixed-convection, skin friction*

Introduction

There is continuous increasing interest of recent researchers in flow problems in magnetized and non-magnetized shapes due to their various applications in industrial and engineering work. Convective heat transfer has various applications in engineering processes like thermal power plants, missiles, heating and cooling processes in semi-conductors electronics, turbo machines, space vehicles, cooling of combustion chamber wall in a gas turbine and nuclear reactors. In the current work, periodic mixed convection 2-D flow around the surface of magnetized cone is considered. Glauert [1] was first who computed a boundary-layer mechanism on magnetized plate analytically. He showed that the boundary-layer separation occurs due to strong magnetic field. Later, Ramamoorthy [2] illustrated a classical theory of heat transfer in boundary-layer along a magnetized plate where magnetic field is applied parallel to the plate. He obtained that temperature in boundary-layer is reduced due to slow movement of fluid by magnetic field. Chawla [3] analyzed oscillating boundary-layer behavior along a magnetized plate numerically. He concluded that amplitude of surface current increases with frequency but phase angle decreases from $90-45^\circ$ angle. Ingham [4] performed a MHD boundary-layer phenomenon over a thermally conducting plate analytically. He obtained that boundary-layer is

* Corresponding author, e-mail: asifa.ilyas@uos.edu.pk

slightly thicker when plate is placed at main stream temperature rather than thermally insulated. Mohanty [5] developed a numerical problem on magnetized plate to predict oscillating magnetic field effects on boundary-layer flow numerically. He observed that magnetic drag decreases due to higher magnetic Prandtl number and then increases with increase in frequency. Chamkha [6] investigated the numerical results of coupled heat and mass transfer of natural-convection flow around the surface of a truncated cone with radiation and magnetic field effects numerically.

Takhar *et al.* [7] developed a numerical problem on transient mixed convection flow around the surface of rotating vertical cone with time-dependent angular velocity in the presence of magnetic field. They observed that the local skin friction in tangential and azimuthal direction increases as angular velocity of cone is increased. An analysis of mixed convection flow around the surface of vertical cone with constant wall temperature has been studied numerically in [8]. It is concluded that the values of the rate of heat transfer gets higher as Prandtl number increases but decreases with magnetic force number. Pullepu and Chamkha [9] considered a numerical problem on mixed convection flow around the surface of vertical cone with non-uniform surface heat flux under the influence of magnetic field applied normal to the cone surface. They neglected the Hall effects of MHD and pressure gradient in given model. Mahmood *et al.* [10] studied the hydromagnetic-flow past a wedge with permeable surface by assuming a constant transpiration through the wedge surface numerically. They noted that the momentum and magnetic boundary-layer is reduced by increasing transpiration parameter. Ravindran *et al.* [11] studied the combined effects of thermal diffusion and mass transfer on a steady mixed convection boundary-layer flow over the surface of a vertical cone. Mahdy *et al.* [12] gave an attention study double-diffusive convection with variable viscosity around the surface of a vertical truncated cone in porous media in the presence of magnetic field and radiation effects. They used shooting technique to find results which are in excellent agreement with previously published work. Ashraf *et al.* [13-15] discussed different cases around the surface of magnetized vertical plate numerically. Chamkha and Rashad [16] studied the effect of magnetic field, Soret-Dufour and chemical reaction on heat and mass transfer in mixed convection flow around the surface of a vertical cone numerically. It is noted that increasing the magnetic field leads to reduce the skin friction coefficients in the tangential direction. Patrulescu *et al.* [17] performed a steady mixed convection boundary-layer problem around the surface of a vertical truncated cone in nanofluids and working fluid is considered as water with $Pr = 6.2$. Hayat *et al.* [18] performed a physical problem on heat and mass transfer characteristics around stretching cylinder numerically. The Burger's fluid-flow mechanism around stretched sheet in a thermally stratified medium with magnetohydrodynamics effects has been illustrated numerically in [19]. They noted that the temperature gradient is reduced due to stratification parameter. Hayat *et al.* [20, 21] developed numerical mechanisms of MHD mixed convection flow of thixotropic nanomaterial and Burger's nanofluids in the presence of thermally stratified medium. Ashraf *et al.* [22] and Ashraf and Fatima [23] have explored different heat transfer cases around magnetized shapes numerically. Sudhagar *et al.* [24] computed the magnetic field effects on mixed convection flow model of a nanofluids around the surface of an isothermal vertical cone. Reddy *et al.* [25] worked on MHD heat and mass transfer mechanism of nanofluids over the surface of a vertical cone under convective boundary conditions numerically. They noted that the thermal boundary-layer thickness is increased with the increase in the values of thermophoresis parameter. Authors in [26-29], have discussed the various trends of heat and mass transfer by using some new techniques of solution. Taking idea from [1-5], we obtained a numerical solution for periodic fluid-flow phenomena along the surface of thermally and electrically conducting cone.

The governing model and flow geometry

Considering 2-D boundary-layer fluid-flow phenomena along the surface of thermally and electrically conducting cone is considered. Figure 1 represents distance along the surface is x , the normal y -direction of the surface and the velocities u and v along the xy -direction. The H_x is magnetic field at the surface of cone, H_y is taking normal to the surface of cone and external fluid velocity is $U(x, t)$. Consider dimensionless system of coupled non-linear PDE:

$$\frac{\partial \bar{u}}{\partial \bar{x}} + \frac{\partial \bar{v}}{\partial \bar{y}} = 0 \quad (1)$$

$$\frac{\partial \bar{u}}{\partial \tau} + \bar{u} \frac{\partial \bar{u}}{\partial \bar{x}} + \bar{v} \frac{\partial \bar{u}}{\partial \bar{y}} = \frac{\partial^2 \bar{u}}{\partial \bar{y}^2} + \xi \left(\bar{h}_x \frac{\partial \bar{h}_x}{\partial \bar{y}} + \bar{h}_y \frac{\partial \bar{h}_x}{\partial \bar{y}} \right) + \lambda \bar{\theta} \quad (2)$$

$$\frac{\partial \bar{h}_x}{\partial \bar{x}} + \frac{\partial \bar{h}_y}{\partial \bar{y}} = 0 \quad (3)$$

$$\frac{\partial \bar{h}}{\partial \tau} + \bar{u} \frac{\partial \bar{h}}{\partial \bar{x}} + \bar{v} \frac{\partial \bar{h}}{\partial \bar{y}} - \bar{h}_x \frac{\partial \bar{u}}{\partial \bar{x}} - \bar{h}_y \frac{\partial \bar{u}}{\partial \bar{y}} = \frac{1}{\gamma} \frac{\partial^2 \bar{h}}{\partial \bar{y}^2} \quad (4)$$

$$\frac{\partial \bar{\theta}}{\partial \tau} + \bar{u} \frac{\partial \bar{\theta}}{\partial \bar{x}} + \bar{v} \frac{\partial \bar{\theta}}{\partial \bar{y}} = \frac{1}{\text{Pr}} \frac{\partial^2 \bar{\theta}}{\partial \bar{y}^2} \quad (5)$$

The dimensionlized boundary conditions:

$$\bar{u} = \bar{v} = 0, \quad \bar{h}_y = 0, \quad \bar{h}_x = 1, \quad \bar{\theta} = 1 \quad \text{at} \quad \bar{y} = 0, \quad (6)$$

$$\bar{u} \rightarrow \bar{U}(\tau), \quad \bar{\theta} \rightarrow 0, \quad \bar{h}_x \rightarrow 0 \quad \text{as} \quad \bar{y} \rightarrow \infty$$

In eqs. (1)-(5) with boundary conditions in eq. (6), ξ is magnetic-force parameter, λ – the mixed convection parameter, γ – the magnetic Prandtl number, Pr – the Prandtl parameter, and H_0 is magnetic field intensity exact at the surface:

$$\xi = \frac{\mu H_0^2}{\rho U_\infty^2}, \quad \alpha = \frac{\kappa}{\rho C_p}, \quad \lambda = \frac{\text{Gr}_L}{\text{Re}_L^2}, \quad \text{Re}_L = \frac{U_\infty L}{\nu}, \quad (7)$$

$$\text{Pr} = \frac{\nu}{\alpha}, \quad \text{Gr}_L = \frac{g \beta \Delta T L^3}{\nu^2}, \quad \gamma = \frac{\nu}{\nu_m}$$

Taking $U(\tau) = 1 + \varepsilon e^{i\omega\tau}$ is the stream velocity under $|\varepsilon| \ll 1$, where ε is presenting periodic component with small magnitude and frequency parameter ω . The velocity of fluid, the magnetic velocity and fluid temperature components u , v , h_x , h_y , and θ are in the sum form of steady and unsteady equations:

$$\bar{u} = u_s + \varepsilon u_t e^{i\omega\tau}, \quad \bar{v} = v_s + \varepsilon v_t e^{i\omega\tau}, \quad \bar{h}_x = h_{xs} + \varepsilon h_{xt} e^{i\omega\tau} \quad (8)$$

$$\bar{h}_y = h_{ys} + \varepsilon h_{yt} e^{i\omega\tau}, \quad \bar{\theta} = \theta_s + \varepsilon \theta_t e^{i\omega\tau}$$

By substitute (8) into eqs. (1)-(5) with boundary conditions (6), we can separate steady and unsteady equations by collecting like powers of $O(\varepsilon^0)$ and $O(\varepsilon e^{i\omega\tau})$.

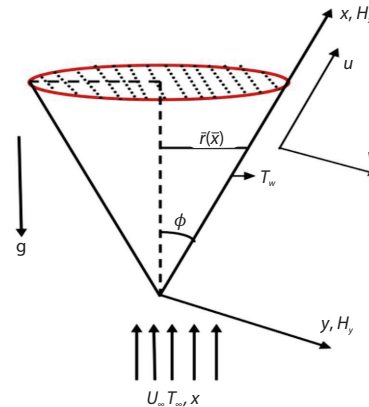


Figure 1. Thermally and electrically conducting cone and co-ordinate system

Computational analysis

The aforementioned obtained dimensionless governing steady, real and imaginary coupled equations are discretized numerically by applying finite-difference scheme, using the Primitive Transformation to obtained primitive form of coupled PDE for further integration. Transformations given in eq. (9) for steady part is used to convert into suitable form both dependent and independent variables:

$$\begin{aligned} u_s(x, y) = U_s(X, Y), \quad v_s(x, y) = x^{-1/2} V_s(X, Y), \quad h_{ys}(x, y) = x^{-1/2} \psi_{ys}(X, Y) \\ h_{xs}(x, y) = \psi_{xs}(X, Y), \quad \theta_s(x, y) = \theta_s(X, Y), \quad Y = x^{-1/2} y, \quad X = x \end{aligned} \quad (9)$$

– For steady equations:

The primitive form of steady equations by using eq. (9), we have:

$$X \frac{\partial U_s}{\partial X} - \frac{Y}{2} \frac{\partial U_s}{\partial Y} + \frac{\partial V_s}{\partial Y} = 0 \quad (10)$$

$$X U_s \frac{\partial U_s}{\partial X} + \left[V_s - \frac{Y}{2} U_s \right] \frac{\partial U_s}{\partial Y} = \frac{\partial^2 U_s}{\partial Y^2} + \xi \left[X \psi_{xs} \frac{\partial \psi_{xs}}{\partial X} + \left(\psi_{ys} - \frac{Y}{2} \psi_{xs} \right) \frac{\partial \psi_{xs}}{\partial Y} \right] + \lambda \theta \quad (11)$$

$$X \frac{\partial \psi_{xs}}{\partial X} - \frac{Y}{2} \frac{\partial \psi_{xs}}{\partial Y} + \frac{\partial \psi_{ys}}{\partial Y} = 0 \quad (12)$$

$$X U_s \frac{\partial \psi_s}{\partial X} + \left[V_s - \frac{Y}{2} U_s \right] \frac{\partial \psi_s}{\partial Y} - X \psi_{xs} \frac{\partial U_s}{\partial Y} - \left(\psi_{ys} - \frac{Y}{2} \psi_{xs} \right) \frac{\partial U_s}{\partial Y} = \frac{1}{\gamma} \frac{\partial^2 \psi_s}{\partial Y^2} \quad (13)$$

$$X U_s \frac{\partial \theta_s}{\partial X} + \left[V_s - \frac{Y}{2} U_s \right] \frac{\partial \theta_s}{\partial Y} = \frac{1}{\text{Pr}} \frac{\partial^2 \theta_s}{\partial Y^2} \quad (14)$$

with boundary conditions:

$$\begin{aligned} U_s = V_s = 0, \quad \psi_{ys} = 0, \quad \psi_{xs} = 1, \quad \theta_s = 1 \quad \text{at} \quad Y = 0 \\ U_s \rightarrow 1, \quad \theta_s \rightarrow 0, \quad \psi_{xs} \rightarrow 0 \quad \text{as} \quad Y \rightarrow \infty \end{aligned} \quad (15)$$

– For real and imaginary equations:

The primitive form of real and imaginary part, by using eq. (16), we have:

$$\begin{aligned} (u_1, u_2) = (U_1, U_2)(X, Y), \quad (v_1, v_2) = x^{-1/2} (V_1, V_2)(X, Y), \quad (h_{y1}, h_{y2}) = x^{-1/2} (\psi_{y1}, \psi_{y2})(X, Y), \\ (h_{x1}, h_{x2}) = (\psi_{x1}, \psi_{x2})(X, Y), \quad (\theta_1, \theta_2) = (\theta_1, \theta_2)(X, Y), \quad Y = x^{-1/2} y, \quad X = x \end{aligned} \quad (16)$$

Using eq. (16) we the find system of coupled non-linear equations in primitive form given:

$$X \frac{\partial U_1}{\partial X} - \frac{Y}{2} \frac{\partial U_1}{\partial Y} + \frac{\partial V_1}{\partial Y} = 0 \quad (17)$$

$$\begin{aligned} X \left[U_s \frac{\partial U_1}{\partial X} + U_1 \frac{\partial U_s}{\partial X} \right] + \left[V_s - \frac{Y}{2} U_s \right] \frac{\partial U_1}{\partial Y} + \left[V_1 - \frac{Y}{2} U_1 \right] \frac{\partial U_s}{\partial Y} - \omega X U_2 = \\ + \frac{\partial^2 U_1}{\partial Y^2} + \xi \left[X \left(\psi_{xs} \frac{\partial \psi_{x1}}{\partial X} + \psi_{x1} \frac{\partial \psi_{xs}}{\partial X} \right) + \left(\psi_{ys} - \frac{Y}{2} \psi_{xs} \right) \frac{\partial \psi_{x1}}{\partial Y} + \left(\psi_{y1} - \frac{Y}{2} \psi_{x1} \right) \frac{\partial \psi_{xs}}{\partial Y} \right] + \lambda \theta_1 \end{aligned} \quad (18)$$

$$X \frac{\partial \psi_{x1}}{\partial X} - \frac{Y}{2} \frac{\partial \psi_{x1}}{\partial Y} + \frac{\partial \psi_{y1}}{\partial Y} = 0 \quad (19)$$

$$X \left[U_s \frac{\partial \psi_1}{\partial X} + U_1 \frac{\partial \psi_s}{\partial X} \right] + \left[V_s - \frac{Y}{2} U_s \right] \frac{\partial \psi_1}{\partial Y} + \left[V_1 - \frac{Y}{2} U_1 \right] \frac{\partial \psi_s}{\partial Y} - \omega X \psi_2 \cdot \\ \cdot \left[X \left(\psi_{xs} \frac{\partial U_1}{\partial x} + \psi_{x1} \frac{\partial U_s}{\partial x} \right) + \left(\psi_{ys} - \frac{Y}{2} \psi_{xs} \right) \frac{\partial U_1}{\partial Y} + \left(\psi_{y1} - \frac{Y}{2} \psi_{x1} \right) \frac{\partial U_s}{\partial Y} \right] = \frac{1}{\gamma} \frac{\partial^2 \psi_1}{\partial Y^2} \quad (20)$$

$$X \left[U_s \frac{\partial \theta_1}{\partial X} + U_1 \frac{\partial \theta_s}{\partial X} \right] + \left[V_s - \frac{Y}{2} U_s \right] \frac{\partial \theta_1}{\partial Y} + \left[V_1 - \frac{Y}{2} U_1 \right] \frac{\partial \theta_s}{\partial Y} - \omega X \theta_2 = \frac{1}{\text{Pr}} \frac{\partial^2 \theta_1}{\partial Y^2} \quad (21)$$

$$X \frac{\partial U_2}{\partial X} - \frac{Y}{2} \frac{\partial U_2}{\partial Y} + \frac{\partial V_2}{\partial Y} = 0 \quad (22)$$

$$X \left[U_s \frac{\partial U_2}{\partial X} + U_2 \frac{\partial U_s}{\partial X} \right] + \left[V_s - \frac{Y}{2} U_s \right] \frac{\partial U_2}{\partial Y} + \left[V_2 - \frac{Y}{2} U_2 \right] \frac{\partial U_s}{\partial Y} + \omega X (U_1) = \frac{\partial^2 U_2}{\partial Y^2} + \\ + \xi \left[X \left(\psi_{xs} \frac{\partial \psi_{x2}}{\partial x} + \psi_{x2} \frac{\partial \psi_{xs}}{\partial x} \right) + \left(\psi_{ys} - \frac{Y}{2} \psi_{xs} \right) \frac{\partial \psi_{x2}}{\partial Y} + \left(\psi_{y2} - \frac{Y}{2} \psi_{x2} \right) \frac{\partial \psi_{xs}}{\partial Y} \right] + \lambda \theta_2 \quad (23)$$

$$X \frac{\partial \psi_{x1}}{\partial X} - \frac{Y}{2} \frac{\partial \psi_{x1}}{\partial Y} + \frac{\partial \psi_{y1}}{\partial Y} = 0 \quad (24)$$

$$X \left[U_s \frac{\partial \psi_2}{\partial X} + U_2 \frac{\partial \psi_s}{\partial X} \right] + \left[V_s - \frac{Y}{2} U_s \right] \frac{\partial \psi_2}{\partial Y} + \left[V_2 - \frac{Y}{2} U_2 \right] \frac{\partial \psi_s}{\partial Y} + \omega X \varphi_1 - \\ - \left[X \left(\psi_{xs} \frac{\partial U_2}{\partial x} + \psi_{x2} \frac{\partial U_s}{\partial x} \right) + \left(\psi_{ys} - \frac{Y}{2} \psi_{xs} \right) \frac{\partial U_2}{\partial Y} + \left(\psi_{y2} - \frac{Y}{2} \psi_{x2} \right) \frac{\partial U_s}{\partial Y} \right] = \frac{1}{\gamma} \frac{\partial^2 \psi_2}{\partial Y^2} \quad (25)$$

$$X \left[U_s \frac{\partial \theta_2}{\partial X} + U_2 \frac{\partial \theta_s}{\partial X} \right] + \left[V_s - \frac{Y}{2} U_s \right] \frac{\partial \theta_2}{\partial Y} + \left[V_2 - \frac{Y}{2} U_2 \right] \frac{\partial \theta_s}{\partial Y} + \omega X \theta_1 = \frac{1}{\text{Pr}} \frac{\partial^2 \theta_2}{\partial Y^2} \quad (26)$$

with boundary conditions:

$$U_1, U_2 = V_1, V_2 = 0, \psi_{y1}, \psi_{y2} = 0, \psi_{x1}, \psi_{x2} = 0, \theta_1, \theta_2 = 0 \quad \text{at } Y = 0 \\ U_1, U_2 \rightarrow 0, \theta_1, \theta_2 \rightarrow 0, \psi_{x1}, \psi_{x2} \rightarrow 0 \quad \text{as } Y \rightarrow \infty \quad (27)$$

The primitive form of equations given in eqs. (17)-(27) is carried out by applying the finite-difference scheme. The numerical results of transformed algebraic expressions with unknown variable U , V , θ , and φ which can be solved in tri-diagonal matrix form by using the Gaussian-elimination scheme for these unknown variables.

Results and discussions

Figures 2(a)-2(c) are plotted against mixed convection, λ , for five choices of values to present numerical results along the surface of a thermally and electrically conducting cone. The amplitude of fluid velocity obtained a certain height for higher value of $\lambda = 7.0$ and good variation at each value in fig. 2(a). The presence of λ exerts buoyancy forces on fluid structure which increases the fluid velocity because λ is the ratio of buoyancy to inertial forces. The char-

acteristics of λ on temperature profile are represented in fig. 2(b). The thermal boundary-layer shows good variations and is increased along the surface of magnetized cone for $\lambda = 0.1$. Also the presence of λ indicates that heat is convected from the surface of magnetized cone to the fluid-flow. The behavior of magnetic profile is illustrated in fig. 2(c) for various values of $\lambda = 0.1, 1.0, 3.0, 5.0,$ and 7.0 . The magnetic profile showed good variations for each value of mixed convection parameter. The magnetic boundary-layer is increased due to slow motion of fluid which generates magnetic current at the surface of cone. This phenomena is valid because the presence of magnetic field produce Lorentz forces which reduce the fluid motion and increase the magnetic boundary-layer thickness along the surface of thermally and electrically conducting cone. The influence of Prandtl number for various values is displayed in figs. 3(a)-3(c). The fluid velocity is maximum at lower $Pr = 1.0$ and good amplitude is observed for each value of Prandtl number in fig. 3(a). The velocity over shoot up to certain height and then asymptotically approached to the given boundary condition. The lower periodic behavior of fluid velocity is seen as Prandtl number increases. It is very important to mention that kinematic viscosity of the fluid increases as Prandtl number increases which increased the momentum boundary-layer thickness along the surface of thermally and electrically conducting cone. Figure 3(b) is sketched for five values of Prandtl number to present the behavior of fluid temperature in given mechanism. The fluid temperature is found to increase for lower Prandtl number and decreases as Prandtl number increases. The similar behavior is observed as Prandtl number is increased. The velocity of magnetic field illustrated variations for each value but similar response for higher values of Prandtl number in fig. 3(c). This is due to reason that the role of Prandtl number in the magnetic field is not very prominent. The phenomena is valid because the fluid become more viscous as Prandtl number increases which results the decrease in fluid motion, so thermal and magnetic boundary-layers are decreased along the surface of thermally and electrically conducting cone. Figures 4(a)-4(c) are presented against various values of γ for fluid velocity, fluid temperature and velocity of magnetic field with some fixed parameters. The periodic amplitude of fluid velocity with good variations is observed for $\gamma = 0.3$ in fig. 4(a) and then asymptotically approaches to given boundary condition. The fluid velocity is maximum at lower magnetic Prandtl number. The good variations in fluid temperature are concluded for each value of γ in fig. 4(b) and thermal boundary-layer showed similar response for higher values of $\gamma = 0.5, 0.7,$ and 0.9 along the surface of cone. The magnetic field effects are observed exact at the surface for various values of γ in fig. 4(c). The magnetic boundary-layer increases for lower magnetic Prandtl number and showed maximum variations for each value. The magnetic Prandtl number has an extensive effect on the results. This phenomena is valid because due to Lorentz force associated with magnetic field increases and it produce more resistance to the transport phenomena. Figures 5(a)-5(c) depict the impact of magnetic force parameter ζ with five choices of numbers on fluid velocity, temperature field and magnetic profile along the surface of thermally and electrically conducting cone. The fluid velocity with certain height and good variations are observed for each value of ζ in fig. 5(a) and then approaches asymptotically to the given boundary conditions. Figure 5(b) demonstrates the same behavior of thermal boundary-layer for each value of ζ and thermal boundary-layer thickness decreases as ζ increases. Magnetic profile illustrate the similar response and minimum variations for increasing ζ . The thermal and magnetic boundary-layers are reduced as ζ increases. It is concluded that increase in magnetic field parameter ζ decelerate the fluid motion which reduced the thermal and magnetic boundary-layer along the surface of thermally and electrically conducting cone. The maximum magnitude of magnetic force parameter is permitting the more fluid to restrict along the surface of thermally and electrically conducting cone.

Velocity of fluid, temperature and magnetic field plots to check the accuracy of the obtained results by boundary conditions

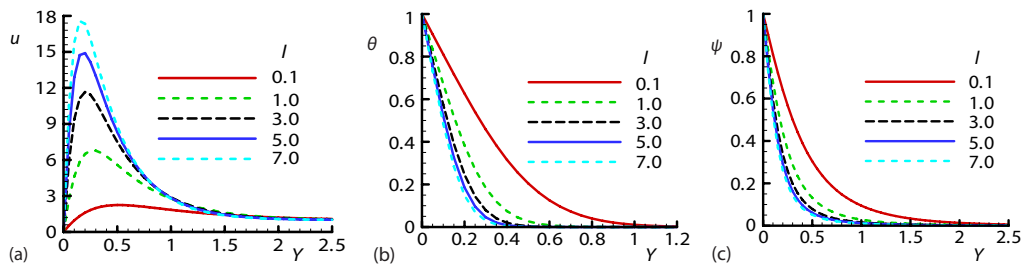


Figure 2. The geometrical profiles for; (a) velocity u , (b) temperature θ , and (c) magnetic field ψ for three choice of $\lambda = 0.1, 1.0, 3.0, 5.0,$ and 7.0 where others are $\gamma = 0.01, Pr = 7.0,$ and $\zeta = 0.2$

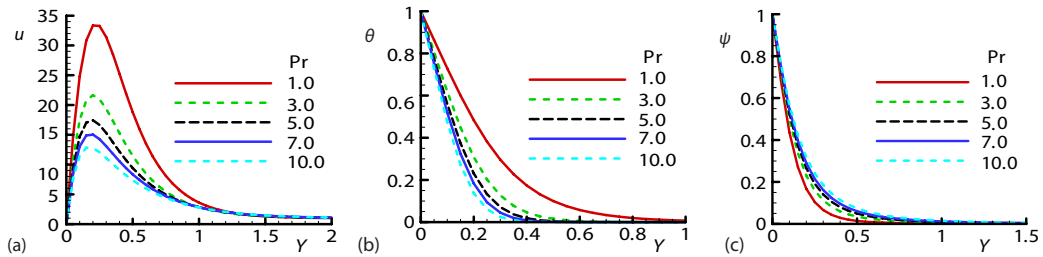


Figure 3. The geometrical profiles for; (a) velocity u , (b) temperature θ , and (c) magnetic field ψ for selected values of $Pr = 1.0, 3.0, 5.0, 7.0,$ and 10.0 while $\gamma = 0.01, \zeta = 0.4,$ and $\lambda = 5.1$

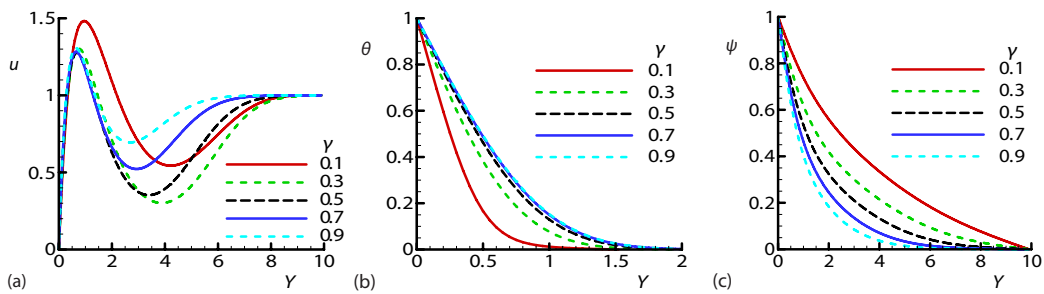


Figure 4. The geometrical profiles for; (a) velocity u , (b) temperature θ , and (c) magnetic field ψ for selected values $\gamma = 0.1, 0.3, 0.5, 0.7, 0.9$ where others are $\lambda = 0.01, \zeta = 30.0,$ and $Pr = 7.0$

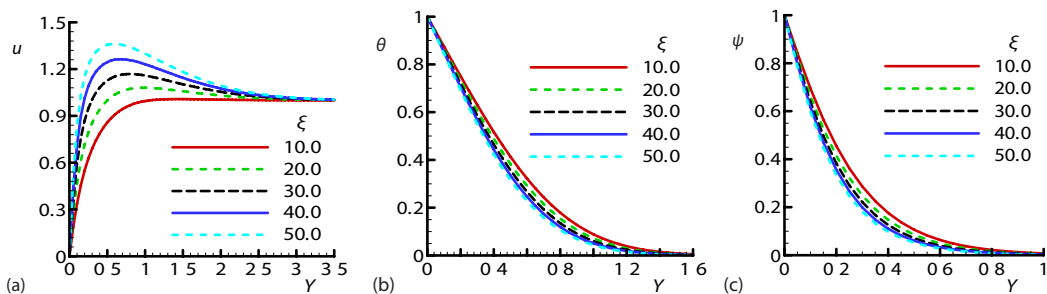


Figure 5. The geometrical profiles for; (a) velocity u , (b) temperature θ , and (c) magnetic field ψ for selected values $\zeta = 10.0, 20.0, 30.0, 40.0, 50.0$ where others are $\lambda = 0.01, Pr = 7.0, \gamma = 0.1$

Figures 6(a)-6(c) are plotted for various values of mixed convection parameter λ to compute periodic quantities of skin friction τ_w , fluctuating heat transfer q_w , and periodic current density j_w along the surface of thermally and electrically conducting cone. The amplitude of τ_w is increased as λ increases in fig. 6(a). The skin friction amplitude is maximum for higher value of λ and good fluctuating response is noted for each value of λ . Figure 6(b) represents the characteristics of periodic heat transfer along the thermally and electrically conducting cone for five values of λ . A good periodic behavior of heat transfer q_w is concluded for each value of λ but maximum oscillations are sketched at $\lambda = 5.0$. The minimum variations for each value of $\lambda = 1.0, 2.0, 3.0, 4.0,$ and 5.0 . but good amplitude for current density j_w is depicted in fig. 6(c). A similar behavior is seen for each value of λ in current density. Because the presence of magnetic field thins the boundary-layer by boosting fluid-flow which enhanced the oscillations in heat transfer in given mechanism. These results are in good agreement because presence of λ is ratio of buoyancy to inertial forces which behave like a wave in fluid and heat transfer characteristics. The physical behavior of emerging parameter Prandtl number with five choices for periodic flow has been drafted in figs. 7(a)-7(c). The highest fluctuating response of skin friction τ_w is noted for lower value of $Pr = 0.1$ in fig. 7(a). The maximum oscillations of τ_w with good variations are concluded for each value of Prandtl number. The amplitude of fluctuating q_w gets higher response for large Prandtl number but very low behavior is seen for lower Prandtl number in fig. 7(b). A good periodic variation trend is observed in heat transfer with good agreement. A similar trend in current density j_w is calculated for every value of Prandtl number but good fluctuation is pointed as Prandtl number increases in fig. 7(c). It is noticed that the amplitude of heat transfer increases as Prandtl number increases but current density decreases for each value of Prandtl number. It can be found that an increase in Prandtl number, increase the specific heat or decrease the thermal diffusivity which causes slower down the oscillation in current density.

Figs. 8(a)-8(c) highlight the impact of increasing magnetic Prandtl parameter γ on periodic fluid-flow mechanism along the cross-section of thermally and electrically conducting cone. The highest amplitude of fluctuations in skin-friction is conducted for increasing $\gamma = 0.5$ but low amplitude is noted for lower $\gamma = 0.1$. Figure 8(b) depicts the same trend of fluctuating heat transfer for five choices of $\gamma = 0.1, 0.2, 0.3, 0.4,$ and 0.5 by keeping some fixed parameters. It is necessary to point out that a very poor variation in the case of periodic heat transfer is examined along the thermally and electrically conducting cone. But a very excellent oscillation in current density is displayed for each value of γ in fig. 8(c). The lower $\gamma = 0.1$ gets poor amplitude in current density but highest amplitude is sketched for higher $\gamma = 0.5$. A very poor response of periodic skin friction, fluctuating heat transfer and periodic current density for five values of magnetic force/field parameter ζ has been drafted in figs. 9(a)-9(c) for given periodic flow along the thermally and electrically conducting cone. From these figures it is extracted that the similar variations with oscillation for each value is examined and very small response is calculated in skin friction.

*Periodic skin friction τ_w ,
heat transfer q_w ,
and current density j_w*

We used solution obtained from steady part into unsteady part and obtain periodic quantities of skin friction, heat transfer and current density.

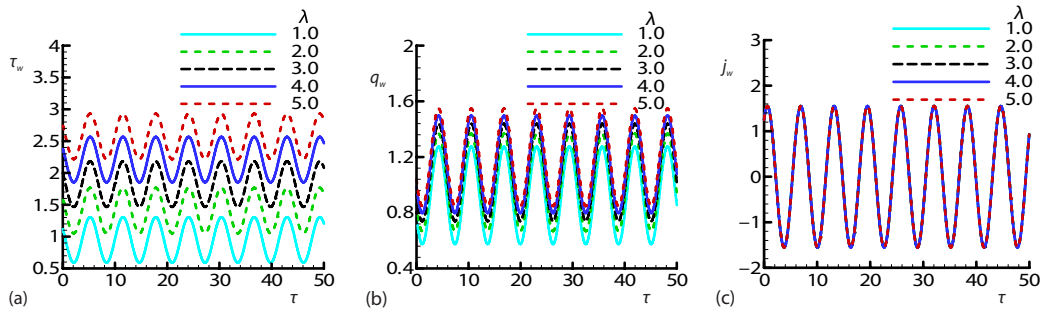


Figure 6. The geometrical profiles of; (a) τ_w , (b) q_w , and (c) j_w for three choice of $\lambda = 1.0, 2.0, 3.0, 4.0, 5.0$ where other parameters $\gamma = 0.8, \zeta = 0.6$, and $Pr = 7.0$

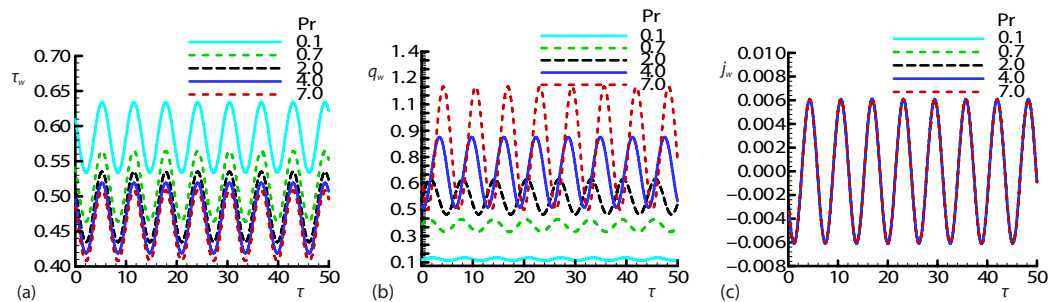


Figure 7. The geometrical profiles of; (a) τ_w , (b) q_w , and (c) j_w for three choice of $Pr = 0.1, 0.7, 2.0, 4.0, 7.0$ where other parameters $\gamma = 0.01, \zeta = 0.2$, and $\lambda = 0.1$

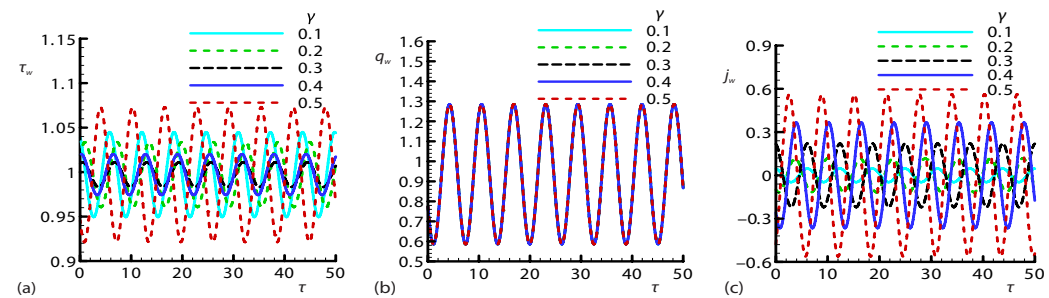


Figure 8. The geometrical profiles of; (a) τ_w , (b) q_w , and (c) j_w for three choice of $\gamma = 0.1, 0.2, 0.3, 0.4, 0.5$ where other parameters $\lambda = 0.01, \zeta = 0.2$, and $Pr = 0.7$ are constant

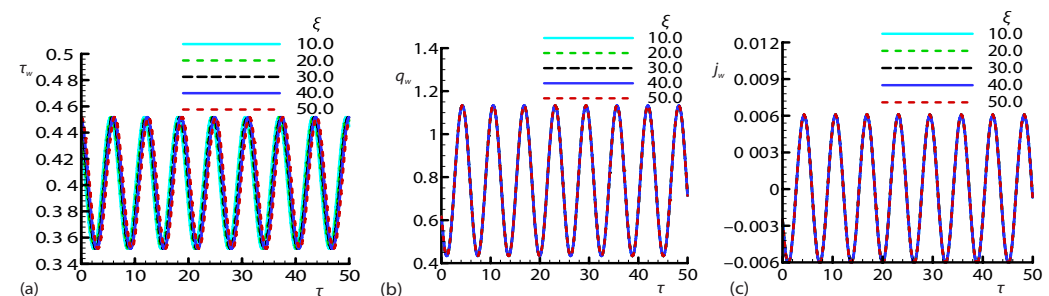


Figure 9. The geometrical profiles of; (a) τ_w , (b) q_w , and (c) j_w for three choice of $\zeta = 10.0, 20.0, 30.0, 40.0, 50.0$ where other parameters $\gamma = 0.01, \lambda = 0.01$, and $Pr = 0.7$ are constant

Conclusion

The present analysis of periodic mixed convection flow and heat transfer characteristics along the surface of thermally and electrically conducting cone have been calculated numerically with primitive variable formulation by applying more efficient finite-difference technique for various governing parameters. To ensure the accuracy of results, the numerical results are plotted against various emerging parameters like mixed convection parameter, λ , magnetic force parameter, ζ , magnetic Prandtl number, γ , and Prandtl number for five choices which are satisfying given boundary conditions. It is depicted that the amplitude of fluid velocity obtained a certain height for higher value of $\lambda = 7.0$ and good variation at each value along the thermally and electrically conducting cone. The fluid temperature is found to increase for lower Prandtl number and decreases as Prandtl number increases. It is also noticed that a good periodic behavior of heat transfer q_w is concluded for each value of λ but maximum oscillations are sketched at $\lambda = 5.0$. It is also computed that the lower $\gamma = 0.1$ gets poor amplitude in current density but highest amplitude is sketched for higher $\gamma = 0.5$. This phenomena is in good agreement because presence of λ exert buoyancy forces which behave like waves in fluid and heat transfer characteristics. It is also noted that due to the increase in magnetic force parameter ζ there are wave like disturbances generate within the fluid layers. These disturbances are basically hydromagnetic waves which becomes more prominent as the strength of magnetic force parameter is increased.

Nomenclature

C_p	– specific-heat, [Jkg ⁻¹ K ⁻¹]
g	– gravitational-acceleration, [ms ⁻²]
Gr_L	– Grashof number
H_x, H_y	– magnetic velocities along x - and y -direction, [Tesla]
j_w	– periodic current density
T	– fluid Temperature, [K]
T_∞	– ambient-temperature, [K]
Pr	– Prandtl number
q_w	– periodic heat transfer
Re	– Reynolds number
u, v	– velocity along x - and y -direction, [ms ⁻¹]

Greek symbols

α	– thermal-diffusivity, [m ² s ⁻¹]
β	– thermal-expansion, [K ⁻¹]
γ	– magnetic-Prandtl parameter
θ	– dimensionized fluid temperature
λ	– mixed convection number
μ	– fluid dynamic viscosity, [kgm ⁻¹ s ⁻¹]
ν	– kinematic-viscosity, [m ² s ⁻¹]
ν_m	– magnetic-permeability, [Hm ⁻¹]
ζ	– magnetic force number
ρ	– fluid density, [kgm ⁻³]
τ	– shearing stress, [Pa]
τ_w	– periodic skin friction

References

- [1] Glauert, M. B., The Boundary-Layer on a Magnetized Plate, *Journal Fluid Mech.*, 12 (1962), 4, pp. 625-638
- [2] Ramamoorthy, P., Heat Transfer in Hydromagnetics, *The Quarterly J. Mech. Appl. Math.*, 18 (1965), 1, pp. 31-40
- [3] Chawla, S. S., Fluctuating Boundary-Layer on a Magnetized Plate, *Proc. Camb. Phil. Soc.*, 63 (1967), 2, pp. 513-525
- [4] Ingham, D. B., The Magnetogasdynamic Boundary-Layer for a Thermally Conducting Plate, *The Quarterly J. Mech. Appl. Math.*, 20 (1967), 3, pp. 347-364
- [5] Mohanty, H. K., The Effects of Magnetic Field Oscillations on the Boundary-Layer Flow Past a Magnetized Plate, *Journal Appl. Math. Phys.*, 23 (1972), Mar., pp. 325-332
- [6] Chamkha, A. J., Coupled Heat and Mass Transfer by Natural-Convection about a Truncated Cone in the Presence of Magnetic Field and Radiation Effects, *Numerical Heat Trans Part A: Applications.*, 39 (2001), 5, pp. 511-530
- [7] Takhar, H. S., et al., Unsteady Mixed Convection Flow from a Rotating Vertical Cone with a Magnetic Field, *Heat. Mass. Trans.*, 39 (2003), 4, pp. 297-304

- [8] Pop, I., et al., Mixed Convection along a Vertical Cone for Fluids of any Prandtl Number: Case of Constant wall temperature, *Int. J. Num. Method. Heat. Fluid. Flow.*, 13 (2003), 7, pp. 815-829
- [9] Pullepu, B., Chamkha, A. J., Transient Laminar MHD Free Convective Flow Past a Vertical Cone with Non-Uniform Surface Heat Flux, *Non-Lin. Anal: Mod. Cont.*, 14 (2009), 4, pp. 489-503
- [10] Mahmood, M., et al., Hydromagnetic-Flow of Viscous Incompressible Fluid Past a Wedge with Permeable Surface, *Z. Angew. Math. Mech.*, 89 (2009), 3, pp. 174-188
- [11] Ravindran, R., et al., Effects of Injection (Suction) on a Steady Mixed Convection Boundary-Layer Flow over a Vertical Cone, *Int. J. Num. Method. Heat. Fluid. Flow.*, 19 (2009), 3-4, pp. 432-444
- [12] Mahdy, A., et al., Double-Diffusive Convection with Variable Viscosity from a Vertical Truncated Cone in Porous Media in the Presence of Magnetic Field and Radiation Effects, *Computer. Math. App.*, 59 (2010), 12, pp. 3867-3878
- [13] Ashraf, M., et al., Thermal Radiation Effects on Hydromagnetic Mixed Convection Flow along a Magnetized Vertical Porous Plate, *Mathematical Problems in Engineering*, 2010 (2010), 686594
- [14] Ashraf, M., et al., Computational Study of Combined Effects of Conduction-Radiation and Hydromagnetics on Natural-Convection Flow Past Magnetized Permeable Plate, *Appl. Math. Mech. Engl. Ed.*, 33 (2012), 6, pp. 731-748
- [15] Ashraf, M., et al., Fluctuating Hydromagnetic Natural-Convection Flow Past a Magnetized Vertical Surface in the Presence of Thermal Radiation, *Thermal Science*, 16 (2012), 4, pp. 1081-1096
- [16] Chamkha, A. J., Rashad, A. M., Unsteady Heat and Mass Transfer by MHD Mixed Convection Flow from a Rotating Vertical Cone with Chemical Reaction and Soret and Dufour Effects, *Canad. J. Chem. Eng.*, 92 (2013), 4, pp. 758-767
- [17] Patrulescu, F. O., et al., Mixed Convection Boundary-Layer Flow from a Vertical Truncated Cone in a Nanofluid, *International Journal of Numerical Methods for Heat and Fluid-Flow*, 24 (2015), 5, pp. 1175-1190
- [18] Hayat, T., et al., Convective Heat and Mass Transfer in Flow by an Inclined Stretching Cylinder, *Journal Mol. Liq.*, 220 (2016), Aug., pp. 573-580
- [19] Hayat, T., et al., The MHD Mixed Convection Flow of Burger's Fluid in a Thermally Stratified Medium, *Journal Aerospace. Eng.*, 29 (2016), 6, pp. 1-7
- [20] Hayat, T., et al., Mixed Convection Flow of a Burgers Nanofluid in the Presence of Stratifications and Heat Generation/Absorption, *Europ. Phys. J. Plus.*, 131 (2016), Aug., pp. 253
- [21] Hayat, T., et al., Analysis of Thixotropic Nanomaterial in a Doubly Stratified Medium Considering Magnetic Field Effects, *Int. J. Heat. Mass. Trans.*, 102 (2016), Nov., pp. 1123-1129
- [22] Ashraf, M., et al., Effects of Temperature Dependent Viscosity and Thermal Conductivity on Mixed Convection Flow Along a Magnetized Vertical Surface, *Int. J. Num. Methods. Heat. Fluid. Flow.*, 26 (2016), 5, pp. 1580-1592
- [23] Ashraf, M., Fatima, A., Numerical Simulation of the Effect of Transient Shear Stress and Rate of Heat Transfer around Different Position of Sphere in the Presence of Viscous Dissipation, *Journal Heat. Trans.*, 140 (2018), 6, 061701
- [24] Sudhagar, P., et al., Magnetohydrodynamics Mixed Convection Flow of a Nanofluid in an Isothermal Vertical Cone, *Journal of Heat Transfer*, 139 (2017), 3, 034503
- [25] Reddy, P. S., et al., Magnetohydrodynamic (MHD) Boundary-Layer Heat and Mass Transfer Characteristics of Nanofluid over a Vertical Cone under Convective Boundary Condition, *Propulsion Power Research*, 7 (2018), 4, pp. 308-319
- [26] Akgul, A., et al., New Method for Investigating the Density Dependent Diffusion NAGUMO Equation, *Thermal Science*, 22 (2018), Suppl. 1, pp. S143-S152
- [27] Inc, M., et al., Modified Variational Iteration Method for Straight Fins with Temperature Dependent Thermal Conductivity, *Thermal Science*, 22 (2018), Suppl. 1, pp. S229-S236
- [28] Kilicman, A., et al., Analytical Approximate Solution for Fluid-Flow in the Presence of Heat and Mass Transfer, *Thermal Science*, 22 (2018), Suppl. 1, pp. S259-S264
- [29] Partohaghigh, M., et al., Fictitious Time Integration Method for Solving the Time Fractional Gas Dynamic Equation, *Thermal Science*, 23 (2019), Suppl. 6, pp. S2009-S20016